Theor Appl Climatol
DOI 10.1007/s00704-017-2150-5

ORIGINAL PAPER

Drought characteristics and prediction during pasture growing season in Xilingol grassland, northern China

Qiyun Ma[1] · Jiquan Zhang[1] · Caiyun Sun[1] · Feng Zhang[1] · Rina Wu[1] · Lan Wu[1]

Received: 5 January 2016 / Accepted: 2 May 2017

Abstract In this paper, spatiotemporal variability of drought in Xilingol grassland during pasture growing season (from April to September) was investigated, using 52 years (1961–2012) of precipitation data recorded at 14 rain gauge stations in the study area. The Standardized Precipitation Index was used to compute the severity of drought. The Mann-Kendall test, the linear trend, and the sequential Mann-Kendall test were applied to standardized precipitation index (SPI) time series. The results indicate that drought has become increasingly serious on the region scale during pasture growing season, and the rate of SPI decreases ranged from −0.112 to −0.013 per decade. As for the MK test, most of the stations, the Z value range is from −1.081 to −0.005 and Kendall's τ varies from −0.104 to −0.024. Meanwhile, drought is increased obviously from the northwest to the southeast region. Meanwhile, the occurrence probability of each severity class, times for reaching different drought class from any drought severity state, and residence times in each drought class have been obtained with Markov chain. Furthermore, the drought severities during pasture growing season in 2013–2016 are predicted depending on the weighted Markov chain. The results may provide a scientific basis for preventing and mitigating drought disaster.

Keywords Meteorological drought · Drought characteristics · Weighted Markov chain · Drought prediction · Xilingol grassland

✉ Jiquan Zhang
zhangjq022@nenu.edu.cn

[1] Institute of Natural Disaster Research, School of Environment, Northeast Normal University, Changchun 130024, People's Republic of China

1 Introduction

Global climate models predict an increase in temporal variability of precipitation and more intense and frequent extreme weather and climate events, such as droughts (IPCC 2007; Cherwin and Knapp 2012; Asadi Zarch et al. 2015). Many definitions of drought exist in the literature. The meteorological drought, which is defined as a lack of precipitation over a region for a period of time (Ashraf and Routray 2015; American Meteorological Society 2004), is utilized in the present study. And, drought is also recognized as one of the most serious natural disasters due to its great damages to people's life, water resources, agricultural production, and natural ecosystem (Smith et al. 2014; Meehl et al. 2000; Sun et al. 2015; Krishnamurthy et al. 2014; Tall et al. 2013). The frequency, duration, and severity of drought have increased substantially in recent decades, affecting large areas in Asia, Europe, Africa, Australia, and America (Mishra and Singh 2010). In northern China, the arid and semi-arid grassland are at the core of livestock and bear vital social, economic, and ecological values. However, the extreme climate of the region is projected to become even more so in the future (Sun et al. 2003), and its bad effects on the regional biogeochemical cycle will be more strongly (Sheffield and wood 2012; Lei et al. 2015).

In grassland ecosystem, droughts will exert an adverse impact on plant growth, structure, composition, and ecosystem functions, particularly aboveground net primary productivity (Jentsch et al. 2011; Xia et al. 2014). In addition, water stress can affect pasture nutritive value and accelerate leaf senescence, both of which contribute to the decline in the pasture quality (Küchenmeister et al. 2013; Bruinenberg et al. 2002; Halim et al. 1989; Jensen et al. 2010; Lei et al. 2015). Therefore, having a better understanding in spatial and temporal characteristics of drought and predicting its occurrence

Published online: 07 June 2017

during the pasture growing season are essential and worthwhile for regional livestock farming. To date, the literature on historical data-based hydroclimatic studies of spatial and temporal characteristics is particularly rich, especially in the area of precipitation and temperature trend analysis (Michaelides et al. 2009; Wang et al., 2015a; Sung et al. 2015). Within the current studies, some methods have used to identify and evaluate the trends during specific periods in various regions, such as linear regression approaches, and the Mann-Kendall test; for instance, see Martinez et al. (2012) and Marofi et al. (2012). The sequential Mann-Kendall test has also been used to analyze of the abrupt change in the long-term time series of climatic dataset (Hosseinzadeh Talaee et al. 2014).

At the same time, drought has a slow initiation and it is usually recognized when the drought is already established (Wilhite and Glantz, 1987; Ashraf and Routray 2015). In this context, prediction of drought is a tough task due to its large-scale impact, and it is vital for decision and policy makers to timely implement policies and measures to mitigate the bad effects of drought. Recently, some efforts have focused on forecasting the natural and human emergency or abnormal situations by constructing systems and using fuzzy mathematical theory (Naderpour et al. 2014, 2015; Purba et al. 2014; Zhang et al., 2012). When it comes to drought, massive attention has been paid to analyze the temporal and spatial variations of drought, and based on this, researchers predict the occurrence of drought with various probabilistic methods based on precipitation probabilities (Steinemann 2006; Lazri et al. 2015). Among these methods, as an improved tool for early warning (Lohani and Loganathan 1997), Markov chain is commonly utilized for investigating the drought characteristics and prediction of drought occurrence by combining drought indices at present (Paulo and Pereira 2007, 2008; Chattopadhyay et al. 2012; Yeh et al. 2015). But, precipitation is a dependent stochastic variable (Sun et al. 2003), and it is always rarely concerned in current research literatures, which may lead to an inaccurate result of drought prediction. Thus, this study aims at providing more reliable and rational results for regional drought prediction by using weighted Markov chain considered the autocorrelation of the precipitation events and the stochastic property of drought.

Xilingol grassland is one of the very backbones for the sustainable development of the economy and ecology in northern China. The animal husbandry and dairy farming here are undeveloped, as a consequence of the harsh natural conditions (Wu et al. 2008). During the past decades, the grasslands have been seriously deteriorating under the combined effects of climate change, land use change, and socioeconomic transformation (Qi et al. 2012; Hao et al. 2014). However, some studies have been concerned about drought in this region, and they focused on the change trends of annual and seasonal precipitation; the studies on the evolution of drought and its prediction during pasture growing season are quite rare. Accordingly, the key objectives of this study are to (1) investigate the spatial and temporal variability of drought in Xilingol during the pasture growing season in 1961–2012; (2) explore the stochastic characteristics of drought, including the occurrence probability of each severity class, times for reaching different drought class from any drought severity state, and residence times in each drought class; and (3) predict the drought severity during pasture growing season in the next few years. Such a study is necessary for protecting vulnerable grassland ecosystem, for water resource management, drought risk assessment, and regional sustainable development in Inner Mongolia (Paulo and Pereira 2008; Zhang et al. 2009).

2 Study area and dataset

The Xilingol grassland (111°59′–120°00′E and 42°32′–46°41′E) is situated in the middle part of the Inner Mongolia Autonomous Region, northeast of China (Fig. 1). It is the most complete wild grassland in the grassland subzone of East Asia in the Eurasian steppe region, with an area of approximately 200,000 km^2, of which the grassland area is 97.8% of the total area. The vegetation types include various formations of desert steppes, typical steppes, and meadow steppes (Liu et al. 2002). It is characterized by having a mid-temperature semi-arid continental climate type. The average annual precipitation in this area ranges from 135 mm in the northwestern to 380 mm in the southeastern. Recently, with the effects of global warming, drought hazards have noticeably increased in this region which have seriously affected the life of the local people living on natural livestock breeding (Gao et al. 2013). Local government and grassland managers have paid great attention to the current and future grassland drought scenarios.

The monthly precipitation observations are obtained from the China Meteorological Data Sharing Service System (http://cdc.cma.gov.cn/). Fourteen rain gauges are selected and have a strict processing and quality control for the period from 1961 to 2012. The pasture growing season is generally from April to September (Li et al. 2013), due to its climate conditions, such as temperature and precipitation. The geographical positions of the selected stations and main characteristics of rainfall data during pasture growing season are presented in Fig. 1 and Table 1.

3 Methodology

3.1 Standardized precipitation index

To assess the evolution of drought severity, researchers have developed many drought indices, which are derived from precipitation or other climatic variables. Among the drought

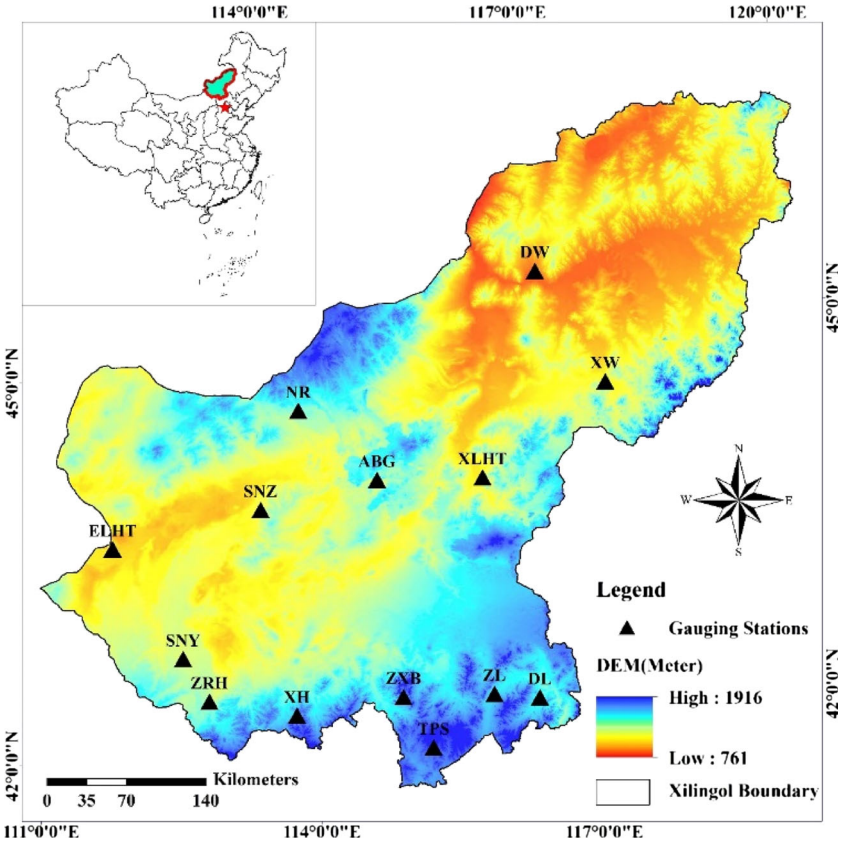

Fig. 1 Location of the study area and rain gauges within Xilingol grassland

indices, standardized precipitation index (SPI) has become a worldwide tool in drought monitoring and forecasting (Heim 2002; Du et al. 2013). It was proposed by McKee et al. (1993) and conceived to identify drought events and the severity of droughts at multiple time scales, for instance, ranging from 1 to 24 months. Shorter and longer time units reflect natural lags in the response of different water resources to precipitation anomalies (Paulo et al. 2005). The SPI, which only considers

Table 1 Location of the stations and characteristics of rainfall data during pasture growing season (1961–2012)

Site	Latitude (E)	Longitude (N)	Elevation (m)	Mean (mm)	Median (mm)	Max (mm)	Min (mm)	C.V (%)	Skewness
ELHT	43°38′	111°58′	964.7	121.1	112.2	239.8	32.5	36.9%	0.79
DW	45°31′	116°58′	838.9	224.7	213.8	435.9	125.3	30.3%	0.94
NR	44°37′	114°09′	1181.6	204.4	199.1	390.2	98.4	31.6%	0.76
ABG	44°01′	114°57′	1126.1	215.1	206.8	421.4	117.8	28.1%	0.65
SNZ	43°52′	113°38′	1036.7	165.3	154.0	259.2	85.1	28.0%	0.16
ZRH	42°23′	112°54′	1150.8	185.0	186.7	317.4	66.0	31.4%	0.15
XW	44°35′	117°35′	995.9	292.7	278.4	530.5	124.5	27.8%	0.61
XLHT	43°57′	116°06′	1003.0	247.4	233.3	457.2	108.4	32.5%	0.71
DL	42°10′	116°28′	1245.4	337.8	335.9	476.8	211.6	20.1%	0.03
SNY	42°45′	112°39′	1103	158.3	159.9	296.3	61.7	30.0%	0.17
XH	42°13′	113°49′	1322.8	229.8	228.2	391.0	101.0	28.7%	0.25
ZL	42°15′	115°58′	1301	327.9	326.1	513.9	181.8	24.8%	0.20
ZXB	42°17′	115°00′	1347.8	307.1	309.3	471.2	178.3	23.5%	0.10
TPS	41°52′	115°16′	1468.7	340.1	337.2	530.0	201.0	23.1%	0.20

ELHT Erenhot, *DW* East Ujimqin Banner, *NR* Narenbaolige, *ABG* Abaga Banner, *SNZ* Sonid Left Banner, *ZRH* Zhurihe, *XW* West Ujimqin Banner, *XLHT* Xilinhot, *DL* Duolun county, *SNY* Sonid Right Banner, *XH* Boarder Yellow Banner, *ZL* Zhenglan Banner, *ZXB* Zhengxiangbai Banner, *TPS* Taibus Banner

precipitation, could be used in any location based on the precipitation record of at least 30 years for a desired period (Ashraf and Routray 2015). Besides, it is a normalized index which permits comparisons of its values among different locations in the world.

The record of long-term precipitation is fitted to a probability distribution and then transformed into a standard normal distribution so that the mean SPI for the interested period is zero (Edwards and McKee 1997). The positive SPI values indicate greater than the average precipitation and vice versa. The drought monthly severity adopted in this study is defined (Table 2), which was modified according to the reality of local climate conditions and where the severe and extremely severe drought classes are grouped. The term near normal, instead of mild drought, is used for better reflecting the fact that this drought classification corresponds to a dry condition identifying a possible initiation or end of a drought period (Paulo and Pereira 2008).

3.2 Mann-Kendall test

The Mann-Kendall (MK) test (Kendall 1955; Mann 1945) is a rank-based non-parametric method, which is applied in this work to detect the existence of significance trends in the time series of SPI. It has been widely used in long-term trend analysis of climatic and hydrologic time series (Tabari et al. 2015; Viola et al. 2014; Golian et al., 2015; Degefu and Bewket 2014). Under the null hypothesis H_0 that a series $\{x_0, \cdots, x_N\}$ comes from where the random variables are independent and identically distributed, the S -statistic of the MK test is calculated as follows:

$$S = \sum_{i=1}^{N-1}\sum_{j=i+1}^{N} sgn\left(x_j - x_i\right) \tag{1}$$

where

$$\mathrm{sgn}\left(x_j - x_i\right) = \begin{cases} 1, x_j > x_i \\ 0, x_j = x_i \\ -1, x_j < x_i \end{cases} \tag{2}$$

x_i and x_j are the sequential data values, and N is the length of the series. Kendall's τ, which measures the strength of the monotonic trend (Wang et al., 2015b), is estimated by

$$\tau = \frac{2S}{N(N-1)} \tag{3}$$

The variance of S is obtained through $\mathrm{var}(S) = N(N-1)(2N+5)/18$. The MK statistic Z is given by

$$Z = \begin{cases} (S-1)/\sqrt{\mathrm{var}(S)}, S > 0 \\ 0, S = 0 \\ (S+1)/\sqrt{\mathrm{var}(S)}, S < 0 \end{cases} \tag{4}$$

The Z values are approximately standard and normally distributed, and trend results have been evaluated at a 0.05 significance level, in which the null hypothesis of no trend is rejected if $|Z| > 1.96$.

For a series with given N, we can compute its var(S), and, at a given significance level, we know its corresponding critical value of Z, ; thus, the corresponding statistic S and the critical value of Kendall's τ will be calculated consequently. The positive values of Kendall's τ indicate increasing trend and vice versa. A completed description of Kendall's τ computation can be found in Wang et al. (2015b).

By checking the SPI time series during the pasture growing season, the autocorrelation is found negligible. Therefore, no preprocessing procedure is applied here. The Kendall's τ of MK trend test for SPI time series is spatially interpolated with the method of inverse distance weighted interpolation (IDW), for the sake of making the spatial characteristics viewed intuitively. This method is a simple deterministic interpolation, which is used for mapping the spatial extent of precipitation trend and drought from point data (Ashraf and Routray 2015).

3.3 Sequential Mann-Kendall test

In this study, the Sequential Mann-Kendall (SQMK) test (Sneyers 1990) is used for detecting the beginning of any significant change in the precipitation time series. It is generally applied to detect the change point in hydroclimatic variables, which has been attracting a number of researchers (Hosseinzadeh Talaee et al. 2014; Jones et al. 2015). It sets up two series, a progressive one of $u(t)$ and a backward one of $u'(t)$. The sequential values of the statistic $u(t)$ are calculated as follows:

$$u(t) = \frac{t_j - E\left(t_j\right)}{\sqrt{var\left(t_j\right)}} \tag{5}$$

in which

$$t_j = \sum_1^j n_j \tag{6}$$

$$E(t) = \frac{n(n-1)}{4}, var(tj) = \frac{j(j-1)(2j+5)}{72} \tag{7}$$

Table 2 Drought severity classification of SPI (modified from McKee et al. 1993)

State (or class)	Drought severity	SPI values
1	Non-drought	SPI > 0
2	Near normal	−1 < SPI ≤ 0
3	Moderate	−1.5 < SPI ≤ −1
4	Severe/extreme	SPI ≤ −1.5

where n_j represents for each element $j(j > i)$ the number of cases $x_j > x_i$ $(j = i+1, \cdots, n$ and $i = 1, \cdots, j-1)$. Computed are the $u(t)$ values from the beginning to the end year of the series, while the values of $u'(t)$ are calculated backward. Ultimately, by plotting the $u(t)$ and $u'(t)$ curves versus time, the approximate time of progressive trend occurrence can be identified by locating the intersection of the curves. If the point at which the two curves intersect is within the upper and lower confidence limits, the detected trend has changed significantly at this point. Moreover, the parts of the curves that exceed the confidence interval indicate the time domain of the abrupt change.

3.4 Weighted Markov chain

Drought can be treated as stochastic events owing to the random character of their contributing factors (Lazri et al. 2015). According to the nature of the Markov stochastic process, the Markov chains are generally used to estimate drought occurrence probability and to assess and predict the time of initiation for a drought event (Isaacson and Madsen 1976; Ochola and Kerkides 2003; Paulo and Pereira 2008; Yeh et al. 2015). Besides, the Markov chain is divided into two types, homogeneous and non-homogeneous. The homogeneous Markov chain is used in this work, where the advantage is that the possible development of the process is independent on time.

A Markov chain (Çinlar 1975; Paulo and Pereira 2007) is a stochastic process X, such as at any time t, and X_{t+1} is conditionally independent from $X_0, X_1, X_2, \ldots, X_{t-1}$ given X_t; the probability that X_{t+1} takes a particular value j depends on the past only through its latest value X_t:

$$P\{X_{t+1} = j | X_0, X_1, \cdots, X_t\} = P\{X_{t-1} = j | X_t = i\} \forall i, j \in S, t \in \quad (8)$$

It is characterized by a set of states, $S = \{S_0, S_1, \cdots, S_T\}$, and by the transition probability, P_{ij}, between states.

The assignment of each SPI value to a drought category seems adequate to Markov chain modeling. Thus, the transition probability matrix

$$P = [P_{ij}] = P\{X_{t+1} = j | X_t = i\} \quad (9)$$

is computed from the sample, counting the number of times, n_{ij}, where the value of SPI passes from the state i to the state j given by

$$P_{ij} = n_{ij} \Big/ \sum_{i=1}^{S} n_{ij} \quad (10)$$

Since the drought index is dependent random variables, the weighted Markov chain (Peng et al. 2009), in this work, is applied to predict and analyze the future drought state. The weighted Markov chain, a tool developed for the prediction or forecasting of drought, is used to predict the future drought state. It is calculated by regarding the standardized autocorrelation coefficient as weights for various lag times of Markov chain (Gong et al. 2014), due to the method based on the special characteristics of the SPI index being a dependent stochastic variable. The process of weighted Markov chain is outlined briefly below.

The different lag time autocorrelation coefficients of the SPI series, r_k, is calculated as

$$rk = \sum_{l=1}^{n-k} \left(x_l - \overline{x}\right)\left(x_{l+k} - \overline{x}\right) \Big/ \sum_{l=1}^{x} \left(x_l - \overline{x}\right)^2 \quad (11)$$

where x_l is the value of SPI at time t, $\overline{x}$ is the average value of SPI, and n is the length of the time series. Subsequently, r_k is transformed into standardized as the weights of each lag time (the number of steps of the SPI from the state i to state j) by

$$w_k = |r_k| \Big/ \sum_{k=1}^{m} |r_k| \quad (12)$$

In the meantime, the state transition probabilities in different lag times could be calculated through Eq. (10). Then, the weighted sums of each state, the predicted probabilities in the same state, will be regarded as the predicted probability of the SPI value in a certain state:

$$P_i = \sum_{i=1}^{m} w_k P_i^{(k)} \quad (13)$$

where weight w_k is derived by Eq. (25). Ultimately, the state $i = \max(P_i, i \in E)$ is the prediction state in the future by weighted Markov analyses. In other words, the drought severity would be predicted. Overall, the implementation of the prediction process is simulated as Table 3. The verification of the predicted ability of the weighted Markov chain will be discussed in Sect. 4.4.

4 Results

4.1 Analysis of Standardized Precipitation Index based on Mann-Kendall test

In this study, the MK test is employed to analyze the trends for SPI series at all of the stations over the period of 1961–2012. This is done by computing the 6-month SPI based on the sum of precipitation of April to September, i.e., the pasture growing season. The MK trend test is used with a 5% significance level. Moreover, the linear trend is used to an auxiliary method to identify the SPI series containing any trends. Positive and negative values, which respectively represent the trends toward wetter and drier conditions, are detected (Du et al.

Table 3 The schematic of the implementation of the weighted Markov chain (take as an example the prediction of drought state in 2013)

Initial year	State	Lag time	Weight	State 1	State 2	State 3	State 4
2012	2	1	w_1	$P_{21}^{(1)}$	$P_{22}^{(1)}$	$P_{23}^{(1)}$	$P_{24}^{(1)}$
2011	2	2	w_2	$P_{21}^{(2)}$	$P_{22}^{(2)}$	$P_{23}^{(2)}$	$P_{24}^{(2)}$
2010	3	3	w_3	$P_{31}^{(3)}$	$P_{32}^{(3)}$	$P_{33}^{(3)}$	$P_{34}^{(3)}$
2009	4	4	w_4	$P_{41}^{(4)}$	$P_{42}^{(4)}$	$P_{43}^{(4)}$	$P_{44}^{(4)}$
P_i				$\sum w_1 P_{21}^{(1)} + w_2 P_{21}^{(2)} + \cdots + w_4 P_{41}^{(4)}$	$\cdots$	$\cdots$	$\sum w_1 P_{24}^{(1)} + w_2 P_{24}^{(2)} + \cdots + w_4 P_{44}^{(4)}$

2013). The results are presented in Table 4 and spatial interpolated using IDW method as shown in Fig. 2. Almost all the rain gauge stations exhibit decreasing SPI trends based on the MK test and linear trend, except Erenhot (ELHT) and Boarder Yellow Banner (XH). The rate of SPI decrease ranged from −0.112 to −0.013 per decade in Xilingol, the maximum in Zhengxiangbai Banner (ZXB) and the minimum in XH. Although the decreased trend of SPI within all the stations is not significant in statistic sense, the results show that the climate is getting drier over the region, and it is necessary to pay more attention to this climate change.

To identify the spatial difference, we divided the SPI tendency rate of per decade into five parts based on the Natural breaks (Jenks) thresholding method. This method does so by identifying the class breaks that minimize the within-group sum of squared difference, yielding internally homogeneous groups and maximizing the differences among the groups (Jung et al. 2013). After this thresholding procedure, the spatial distribution is shown in Fig. 2. It can be seen that the SPI decreased from northwest to southeast; that is to say, the southeast in Xilingol is becoming drier obviously during pasture growing season. This was also confirmed by other studies (Huang et al. 2015), which found increasing trends of dry conditions in southeastern Inner Mongolia and central Inner Mongolia.

For the Z value and Kendall's τ of the MK test, similar to linear trend, the SPI has displayed decreasing trends at 12 stations. In most of the stations, the Z value range is from −1.081 to −0.245 and Kendall's τ varies from −0.104 to −0.024. The maximum value is located in Narenbaolige (NR) and the minimum is in ZXB. In contrast, the ELHT and the XH rain gauge stations exhibit opposite trends (as bold in Table 4). The results show that these two stations is getting wetter slowly during pasture growing season. Figure 3 shows the spatial difference of Kendall's τ in Xilingol. The characteristics of spatial distribution have no distinct difference comparing with the result of the linear trend test. Since there is substantial variability in the SPI of most of the stations in Xilingol, it can be concluded that the drought trend is becoming more severe.

4.2 Sequential Mann-Kendall test of the standardized precipitation index time series

The SQMK test graphs for each rain gauge station during the pasture growing season are presented in Fig. 4. As seen in these figures, all the station $u(t)$ values are similar to show stable fluctuations from the 1960s to the mid-1990s, then becoming severe in the recent decade years. The change point is detected at six stations, East Ujimqin Banner (DW), Abaga

Table 4 The SPI tendency rate, the MKZ values, and the Kendall's τ of the stations during pasture growing season in Xilingol

Site	SPI tendency rate (/10 years)	Z values	Kendall's τ	Site	SPI tendency rate (/10 years)	Z values	Kendall's τ
ELHT	−0.029	*0.039*	*0.005*	XLHT	−0.098	−1.057	−0.102
DW	−0.036	−0.655	−0.063	DL	−0.055	−0.331	−0.032
NR	−0.023	−0.245	−0.024	SNY	−0.043	−0.537	−0.052
ABG	−0.076	−0.947	−0.091	XH	−0.013	*0.134*	*0.014*
SNZ	−0.082	−0.836	−0.081	ZL	−0.098	−0.900	−0.087
ZRH	−0.067	−1.042	−0.100	ZXB	−0.112	−1.081	−0.104
XW	−0.065	−0.513	−0.050	TPS	−0.059	−0.450	−0.044

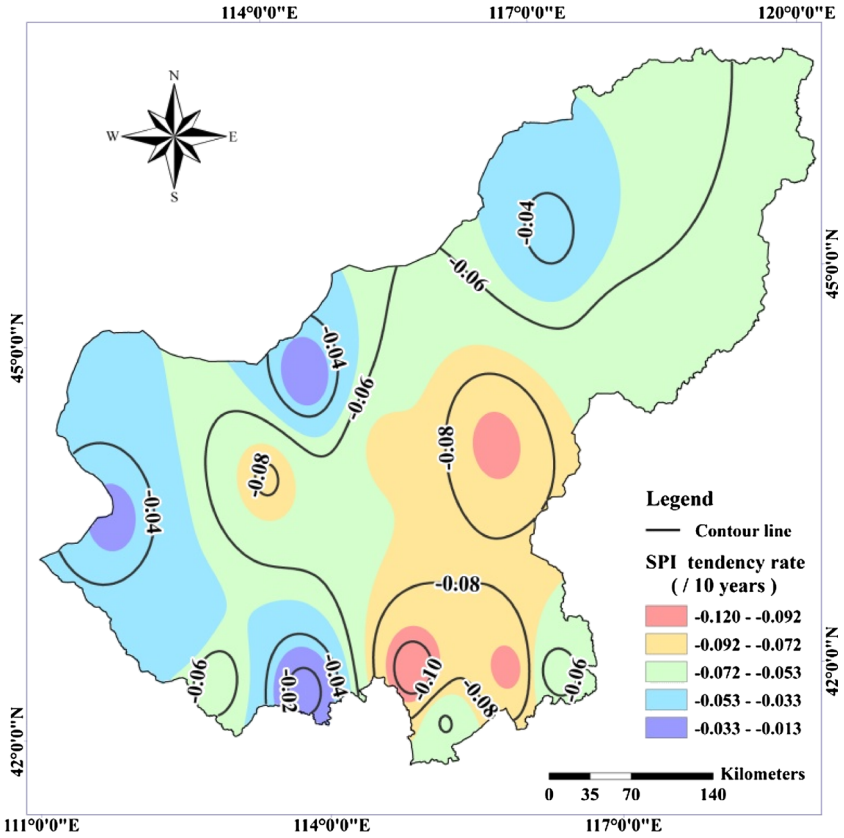

Fig. 2 Distribution of the SPI tendency rate per decade during pasture growing season over Xilingol

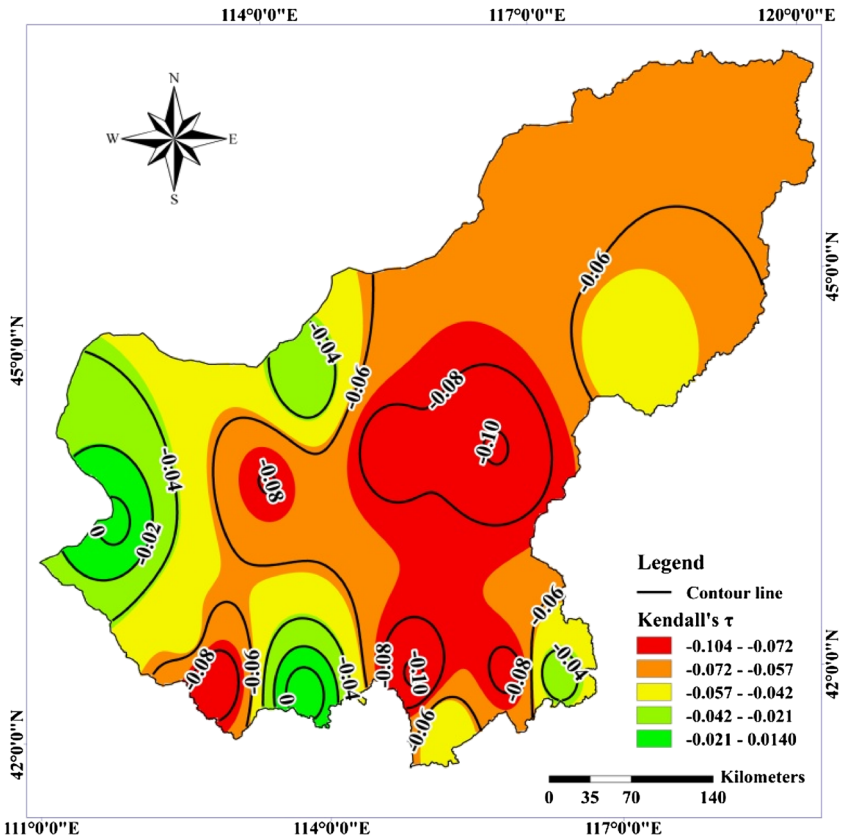

Fig. 3 Spatial distribution of the Kendall's τ during pasture growing season over Xilingol

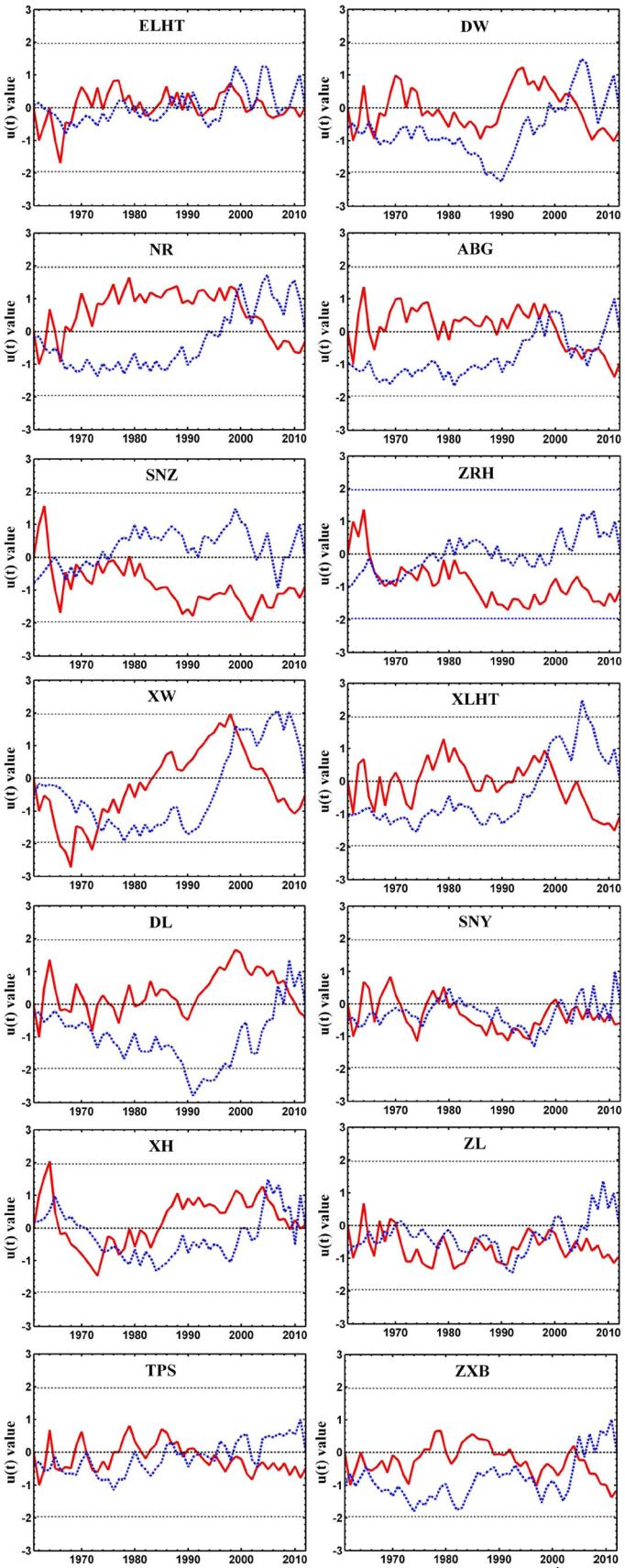

Fig. 4 Sequential MK graphs for SPI series of each station (*blue solid line*: $u(t)$ values; *red dashed line*: $u'(t)$ values; *gray dashed line*: 95% confidence internal limits)

Table 5 Drought class probabilities during pasture growing season

Analytical steady class probabilities

Site	Non-drought	Near normal	Moderate	Severe/extreme	Site	Non-drought	Near normal	Moderate	Severe/extreme
ELHT	0.442	0.442	0.058	0.058	XLHT	0.462	0.404	0.077	0.058
DW	0.462	0.365	0.135	0.038	DL	0.519	0.308	0.038	0.135
NR	0.500	0.288	0.135	0.077	SNY	0.538	0.308	0.077	0.077
ABG	0.481	0.346	0.058	0.115	XH	0.577	0.250	0.096	0.077
SNZ	0.481	0.327	0.115	0.077	ZL	0.519	0.327	0.077	0.077
ZRH	0.558	0.288	0.096	0.058	ZXB	0.577	0.231	0.096	0.096
XW	0.442	0.385	0.096	0.077	TPS	0.500	0.308	0.115	0.077

Banner (ABG), West Ujimqin Banner (XW), Xilinhot (XLHT), Duolun county (DL), XH, and ZXB. The change point of DW occurred in 2003, ABG in 1998, XW in 1973 and 1998, XLHT in 1998, DL in 2009, XH in 1994 and 2005, and ZXB in 2005. These change points and the $u(t)$ value changes are not or not clearly significant in statistic sense. Furthermore, the moving t test, which was used to check the result of the detecting change point, is applied in this study. The moving t test can avoid the disruption by people for the selection of subsequence (Zhao et al. 2007; Li et al. 2014). Combining these two methods, the result could be more reliable and objective. And, the results of the moving t test is similar to the SQMK test; the change years in XW, NR, XLHT, DW, and DL were all in 1998; and DL has other abrupt change years which are in 1992 and 1993. On the whole, the change point during pasture growing season in Xilingol varied between 1992 and 2005.

4.3 Stochastic characteristics of droughts using Markov chain

Table 5 shows that the probabilities of drought severity classes decrease with the degree of severity. ABG and DL are exceptions in which the probability of occurrence of severe/extreme drought categories is higher than the moderate. At the same time, in ELHT, SNY, ZL, and ZXB, the probabilities between stations range from 0.442 in ELHT to 0.577 in XH and ZXB. The relative differences between two different drought classes are higher. For example, the probability of the moderate drought class in DL is 0.058 while in NR, it is more than twice, 0.135; the probability of the severe or extreme drought class in DW is 0.038 while in DL, it is more than three times, 0.135. In total, the respective cumulated probability of drought occurrence, among the drought classes, exceeds 0.50 in most locations, especially in southeastern Xilingol where the SPI decreased more apparently than did any other part of the region discussed in Sect. 4.1. When it refers to the mild drought class, Paulo and Pereira (2007, 2008) stated that it may be replaced by near normal to identify dry but less severe, varying from 0.250 in XH to 0.442 in ELHT.

The expected residence time in each drought severity class represents the average duration of that class expressed in each pasture growing season (Table 6). The duration of drought severity classes decrease with the degree of severity as well. The non-drought class is more persistent, with a duration ranging from 1.47 years in ELHT and SNY to 2.09 years in XW in all locations. All the locations show a similar behavior in the rest of the drought severity classes. It is noteworthy that most of the severe or extreme drought classes persist for 1 year. From Tables 5 and 6, it may be tentatively concluded that drought intensity frequently changes.

The expected first passage time represents the average time period taken by the process to reach for the first time the drought class j starting from some class i. The expected time

Table 6 Expected residence time in each drought severity class during pasture growing season (years)

Site	Non-drought	Near normal	Moderate	Severe/extreme	Site	Non-drought	Near normal	Moderate	Severe/extreme
ELHT	1.47	1.64	1.00	1.00	XLHT	2.00	2.10	2.00	1.00
DW	1.50	1.55	1.17	1.00	DL	2.08	1.45	1.00	1.00
NR	1.53	1.15	1.00	1.00	SNY	1.47	1.45	1.33	1.00
ABG	1.56	1.29	1.17	1.00	XH	2.00	1.44	1.00	1.00
SNZ	1.56	1.31	1.00	1.00	ZL	1.80	1.55	1.00	1.00
ZRH	1.81	1.36	1.00	1.00	ZXB	2.00	1.67	1.25	1.00
XW	2.09	1.67	1.25	1.00	TPS	1.63	1.33	1.20	1.00

Table 7 Expected time to reach the non-drought class from any drought class during pasture growing season (years)

Site	Non-drought	Near normal	Moderate	Severe/extreme	Site	Non-drought	Near normal	Moderate	Severe/extreme
ELHT	2.317	2.025	1.000	1.675	XLHT	2.218	2.449	3.490	2.980
DW	2.218	1.958	1.500	2.000	DL	1.970	2.172	1.000	2.241
NR	2.040	1.659	1.711	1.428	SNY	1.890	1.455	1.333	1.000
ABG	2.056	1.677	1.000	1.735	XH	1.759	1.743	1.349	1.337
SNZ	2.128	1.743	2.111	1.436	ZL	1.961	1.844	1.461	1.826
ZRH	1.821	1.503	1.601	1.534	ZXB	1.757	1.714	1.679	1.343
XW	2.318	2.703	3.865	2.351	TPS	2.041	1.640	1.856	1.820

to reach the non-drought, near-normal, moderate, and severe or extreme class is presented in Tables 7, 8, 9, and 10. Apparently, the higher the drought severity class is, the easier the transfer into the low-level drought severity class, and the non-drought class does not need too much time to reach the more severe drought class. What is more, the self-transfer in the drought severity classes needs more time, such as from the non-drought class to reach the non-drought class in the future; especially, it occurs in higher class as shown in Tables 8, 9, and 10. In general, the drought initiation and establishment is a slower process than drought dissipation (Paulo and Pereira. 2008). It is in line with previous researches. In this study, the occurrence probabilities of the non-drought state are higher and the same as the expected residence time. But, once drought occurs, it will take more time to return to normal on account that self-transfer in drought state needs more time. Thus, these results show that Xilingol grassland is often stricken by droughts, which justifies the desired for improving tools for early warning that may be used for drought risk management both at farm and region scales.

4.4 Prediction of drought class transitions using weighted Markov chain

For the sake of validating the weighted Markov chain ability of drought prediction, this paper compares the true drought state in the 2001–2012 years, which means the identified drought state based on historical precipitation, with the forecasting results as shown in Table 11. On the whole, it shows that the model has a strong predictive ability of non-drought state, and the predicting accuracy rate is up to 95.7%. The next is the class of near normal, in which predicting accuracy rate reaches 75%. The model presents a weak predictive ability of moderate and more severe droughts (class 3 and 4), especially the severe or extreme droughts. Based on the analysis of the correct prediction results, the model predictive capacity is stronger for continuous in the same drought state, while the ability is weak when there is a sharp change or increasing of drought intensity. Namely, when the moderate or more severe drought class occurs abruptly, the weighted Markov chain predictability is a little intractable. However, despite that the predictive results referring to catch the change in drought is not very well, the model still open a window on the prediction of moderate and more severe droughts thanks to the predictive result of the near normal class. The reason is that when the near normal class has been predicted, the probability occurrence of near normal, moderate, and severe or extreme drought class is 75, 50, and 61%, respectively, and the probability occurrence of the non-drought is only 22%. Besides, when the moderate or more severe drought class breaks out, the occurrence of the drought is predicted despite that it is often lower than the real drought severity. And, the predictive ability in each location is almost reached to 67%, even 75%. Hence, as an early warning tool for drought disaster,

Table 8 Expected time to reach the near normal class from any drought class during pasture growing season (years)

Site	Non-drought	Near normal	Moderate	Severe/extreme	Site	Non-drought	Near normal	Moderate	Severe/extreme
ELHT	1.800	2.219	2.800	2.200	XLHT	2.755	2.430	5.204	3.653
DW	2.292	2.688	3.792	4.292	DL	3.554	3.163	4.554	2.523
NR	2.735	3.403	2.563	3.692	SNY	3.182	3.185	4.515	4.182
ABG	2.238	2.955	3.238	3.191	XH	4.086	3.922	4.269	5.131
SNZ	2.629	2.997	2.371	2.971	ZL	3.042	3.000	3.281	3.341
ZRH	3.190	3.400	2.914	4.098	ZXB	5.571	4.252	5.429	5.457
XW	2.811	2.550	1.851	2.405	TPS	2.955	3.188	2.973	2.478

Table 9 Expected time to reach the moderate class from any drought class during pasture growing season (years)

Site	Non-drought	Near normal	Moderate	Severe/extreme	Site	Non-drought	Near normal	Moderate	Severe/extreme
ELHT	16.000	15.475	16.995	16.825	XLHT	27.735	27.061	12.707	19.265
DW	7.000	6.833	7.300	9.000	DL	25.586	27.759	26.604	27.828
NR	6.449	6.068	7.279	5.837	SNY	15.667	17.121	12.739	16.667
ABG	16.469	15.063	17.490	14.094	XH	9.143	9.429	10.206	7.857
SNZ	7.179	7.464	8.488	8.250	ZL	11.671	11.988	12.778	9.832
ZRH	8.724	9.914	10.194	6.816	ZXB	11.071	12.786	10.211	12.414
XW	11.297	11.243	10.198	12.270	TPS	8.712	9.432	8.494	10.072

prediction of drought with the weighted Markov chains can be considered to be feasible.

Ultimately, the drought severities in the next few years, from 2013 to 2016, are predicted as shown in Fig. 5. The result is consistent with the regional drought trends illustrated in Sect. 4.1; for example, in ABG and ZXB, there is an increasing trend of severe drought the same as the MK. In a word, the predictive results can provide a scientific basis for region drought risk management and for governmental decision makers to prevent and mitigate drought disaster during pasture growing season in the future.

5 Discussion

Drought conditions have been measured by the SPI index. Although it has many advantages as described in Sect. 3.1, the limitations are the length of precipitation record and nature of probability distribution (Mishra and Singh 2010). However, the 55-year precipitation data was applied to this study and the Gamma distribution has been taken to calculate the SPI, which can reduce the limitations of the SPI index in a way. Based on the SPI series during the pasture growing season, drought variability has been analyzed using the MK test and the SQMK test. As illustrated in Table 4 and Figs. 2 and 3, a slow dry tendency can be found in the whole region during the pasture growing season. But, the results in ELHT and XH are a little difference based on the two methods, the MK test, and the linear trends. The MK test shows that drought in ELHT and XH seems to have relief from 1961. In contrast, the linear trends show that drought has exhibited increasing trends. It may be caused by intensive climate fluctuations in the latest decade. Likewise, the results presented in Fig. 4 indicate that an abrupt change of drought severities has been identified at some site in 1998. However, the time spell of interest, which means the pasture growing season in this research, may be another influence factor for differences in the length of data using the SPI calculated that may produce considerable impacts on detected trends (Wang et al., 2015b).

Given the dry tendency in Xilingol, it is also confirmed by other studies (Gao et al., 2013), which found increasing trends of dry conditions associated with weakened precipitation in the central and east Inner Mongolia since the 1990s. Additionally, the El Niño-Southern Oscillation (ENSO) and the decline of the Asian monsoonal circulation strength contributed to the drought during the pasture growing season (Huang et al. 2015). Furthermore, the spatial division is achieved in which the more severe area was located at the southeastern Xilingol, where the temperate typical grassland is distributed. It should attract the local government's considerable attention.

Drought characteristics are investigated through the Markov chains. As a result, Xilingol grassland is frequently stricken by droughts with fickle drought severity. Then, by using the weighted Markov chains, the drought severities in 2013–2016 are predicted. The drought characteristics are shown in Tables 5, 6, 7, 8, 9, and 10, and the validation and prediction of the drought severities are listed and displayed in

Table 10 Expected time to reach the severe or extreme class from any drought class during pasture growing season (years)

Site	Non-drought	Near normal	Moderate	Severe/extreme	Site	Non-drought	Near normal	Moderate	Severe/extreme
ELHT	16.175	15.650	17.175	16.995	XLHT	17.837	19.245	10.918	16.972
DW	49.000	48.833	42.000	24.980	DL	6.475	6.033	7.475	7.219
NR	11.440	12.000	12.680	12.749	SNY	11.750	13.205	13.083	12.728
ABG	8.727	8.909	9.727	8.468	XH	11.486	11.771	12.543	12.740
SNZ	11.679	11.964	10.875	12.727	ZL	11.305	11.928	12.461	12.742
ZRH	15.675	15.614	16.650	17.041	ZXB	8.857	10.571	10.536	10.240
XW	12.122	11.378	9.784	12.752	TPS	11.505	11.996	12.901	12.730

Table 11 The validation of the weighted Markov chain ability of drought prediction during pasture growing season in 2000–2012

Year	ELHT		DW		NR		ABG		SNZ		ZRH		XW		XLHT		DL		SNY		XH		ZL		ZXB		TPS	
	T	*P*	*T*	*P*	*T*	*P*	*T*	*P*	*T*	*P*	*T*	*P*	*T*	*P*	*T*	*P*	*T*	*T*	*T*	*T*	*T*	*P*	*T*	*P*	*T*	*P*	*T*	*P*
2001	4	1	2	1	3	1	4	2	3	1	3	1	3	3	3	1	4	2	3	1	3	2	4	1	2	2	4	1
2002	1	1	1	1	1	1	3	1	2	2	2	2	3	2	3	2	2	2	3	2	1	1	3	2	1	1	2	2
2003	1	1	2	2	1	1	1	1	•	1	1	1	2	2	1	1	1	1	1	1	1	1	1	1	1	1	1	1
2004	2	2	2	2	2	2	2	2	1	1	1	1	1	1	1	1	1	1	1	1	1	1	1	1	1	1	1	1
2005	4	2	3	1	3	1	2	1	4	2	3	1	2	2	4	2	2	2	4	3	3	1	2	2	4	2	2	2
2006	2	1	4	1	2	2	1	1	2	2	2	2	3	2	3	1	1	1	1	1	2	2	1	1	1	2	1	1
2007	1	1	4	3	3	2	2	2	1	1	4	1	4	1	4	2	4	2	4	2	4	2	4	2	4	1	2	1
2008	2	2	1	1	1	1	1	1	2	2	1	1	1	2	2	2	1	1	1	1	1	1	1	1	1	1	1	2
2009	1	1	1	1	2	1	2	2	1	1	2	3	3	2	2	2	4	1	2	2	3	2	4	2	3	2	4	2
2010	2	2	2	2	3	3	4	1	2	1	1	1	2	2	2	2	2	2	1	1	1	1	1	1	1	1	1	1
2011	2	2	2	2	2	1	4	3	3	3	3	2	1	1	2	2	4	1	3	2	2	2	3	2	4	2	4	3
2012	1	1	1	1	1	1	1	1	1	1	1	1	1	1	1	1	2	2	1	1	1	1	1	1	1	1	1	1

T true drought state, *P* predictive drought state, • the predictive result is right

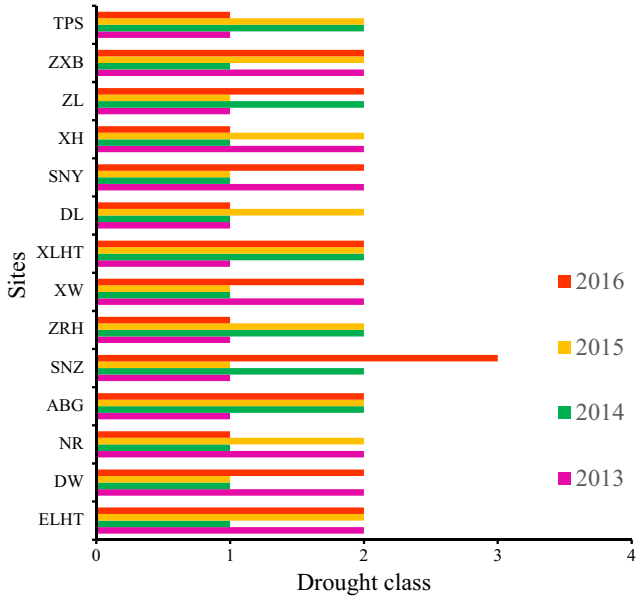

Fig. 5 Drought severity prediction during pasture growing season in 2013–2015

Table 11 and Fig. 5. As mentioned in the previous studies, the Markov transition probability matrices show a strong diagonal tendency in short-term forecasts (Paulo and Pereira 2008), and the weighted Markov chain may reduce the tendency since its prediction is based on the weighted. In spite of the limitations of the weighted Markov chain, once the near normal drought class is predicted, the mitigation and prevention measures are required to be enacted. Thus, these results are promising under a perspective of drought management, particularly referred to drought risk management. However, the methods of drought forecasting need further research. Furthermore, many stochastic models and remote sensing methods should be used together since a combination of predictions from different models may help in confirming the results (Paulo and Pereira 2007) and improving the precision of drought prediction.

6 Conclusion and further study

In the present study, the spatial and temporal characteristics of drought during pasture growing season in Xilingol were surveyed by using SPI as a drought indicator. In general, almost the whole Xilingol grassland was dominated by slow drying tendencies over the years 1961–2012. The spatial distribution analysis of drought is characterized by a general increase from the northwest to southeast region. The abrupt change point was varied between 1992 and 2005 in Xilingol grassland. Furthermore, the Markov chains have been shown to be useful in understanding the stochastic characteristics of drought. The prediction capacity of the weighted Markov chain had been validated, and the drought severities during pasture growing season in 2013–2016 were predicted. The result of the

validation in the model indicated that there was a weak ability to predict moderate or more severe drought. On all accounts, it still could be treated as a scientific basis for water management and drought risk management.

Drought is a pernicious and creeping phenomenon unlike other climatic events. It is affected by both natural conditions and human activities. This study just considers the precipitation as the factors. However, the drought occurrence in grassland will be related with herbage drought resistance, topography of study area, and local anti-drought measures. What is more, the timescale may be adjusted and detailed according to the herbage growth and development stage. These are the limitations of this study, and they will continue to be explored in further studies.

Acknowledgments This study was financially supported by the National Science and Technology Pillar Program during the 12th Five-Year Plan Period No. 2013BAK05B02. The authors are grateful to the anonymous reviewers for their insightful and constructive comments to improve this manuscript.

References

American Meteorological Society (2004) Statement on meteorological drought. Bull Am Meteorol Soc 85:771–773

Asadi Zarch MA, Sivakumar B, Sharma A (2015) Droughts in a warming climate: a global assessment of standardized precipitation index (SPI) and reconnaissance drought index (RDI). J Hydrol 526:183–195

Ashraf M, Routray JK (2015) Spatio-temporal characteristics of precipitation and drought in Balochistan province, Pakistan. Nat Hazards 77(1):229–254

Bruinenberg MH, Valk H, Korevaar H, Struik PC (2002) Factors affecting digestibility of temperate forages from seminatural grasslands: a review. Grass Forage Sci 57(3):292–301

Chattopadhyay S, Acharya N, Chattopadhyay G, Kiran Prasad S, Mohanty UC (2012) Markov chain model to study the occurrence of pre-monsoon thunderstorms over Bhubaneswar, India. Compt Rendus Geosci 344(10):473–482

Cherwin K, Knapp A (2012) Unexpected patterns of sensitivity to drought in three semi-arid grasslands. Oecologia 169(3):845–852

Çinlar E (1975) Introduction to stochastic processes. Prentice-Hall, New Jersey

Degefu MA, Bewket W (2014) Variability and trends in rainfall amount and extreme event indices in the Omo-Ghibe River basin, Ethiopia. Reg Environ Chang 14(2):799–810

Du J, Fang J, Xu W, Shi PJ (2013) Analysis of dry/wet conditions using the standardized precipitation index and its potential usefulness for drought/flood monitoring in Hunan province, China. Stoch Env Res Risk A 27(2):377–387

Edwards DC, McKee TB (1997) Characteristics of 20th century drought in the United States at multiple scales. Atmospheric Science Paper No. 634, May 1–30

Gao T, Yang XC, Jin YX et al (2013) Spatio-temporal variation in vegetation biomass and its relationships with climate factors in the Xilingol grasslands, northern China. PLoS One 8(12):1–10

Golian S, Mazdiyasni O, AghaKouchak A (2015) Trends in meteorological and agricultural droughts in Iran. Theor Appl Climatol 119(3–4):679–688

Gong ZW, Chen CQ, Ge XM (2014) Risk prediction of low temperature in Nanjing city based on grey weighted Markov model. Nat Hazards 71(2):1159–1180

Halim RA, Buxton DR, Hattendorf MJ, Carlson RE (1989) Water-stress effects on alfalfa forage quality after adjustment for maturity differences. Agron J 81:189–194

Hao L, Sun G, Liu YQ et al (2014) Effects of precipitation on grassland ecosystem restoration under grazing exclusion in Inner Mongolia, China. Landsc Ecol 29(10):1657–1673

Heim RR (2002) A review of twentieth-century drought indices used in the United States. Bull Am Meteorol Soc 83:1149

Hosseinzadeh Talaee P, Tabari H, Abghari H (2014) Pan evaporation and reference evapotranspiration trends detection in western Iran with consideration of data persistence. Hydrol Res 45:213–225

Huang J, Xue Y, Sun SL, Zhang JC (2015) Spatial and temporal variability of drought during 1960–2012 in Inner Mongolia, north China. Quatern Int 355:134–144

IPCC (2007) Climate change 2007: the physical Science basis. Contribution of working group I to the fourth assessment report of the intergovernmental panel on climate change. Cambridge University Press, Cambridge, United Kingdom and New York, NY, USA

Isaacson DL, Madsen R (1976) Markov chains: theory and applications. Wiley, New York

Jensen KB, Waldron BL, Peel MD, Robins JG (2010) Nutritive value of herbage of five semi-irrigated pasture species across an irrigation gradient. Grass Forage Sci 65(1):92–101

Jentsch A, Kreyling J, Elmer M et al (2011) Climate extremes initiate ecosystem-regulating functions while maintaining productivity. J Ecol 99(3):689–702

Jones JR, Schwartz JS, Ellis KN, Hathaway JM, Jawdy CM (2015) Temporal variability of precipitation in the upper Tennessee Valley. Journal of Hydrology: Regional Studies 3:125–138

Jung J, Kim C, Jayakumar S et al (2013) Forest fire risk mapping of Kolli Hills, India, considering subjectivity and inconsistency issues. Nat Hazards 65(3):2129–2146

Kendall MG (1955) Rank correlation methods. Griffin, London

Krishnamurthy PK, Lewis K, Choularton RJ (2014) A methodological framework for rapidly assessing the impacts of climate risk on national-level food security through a vulnerability index. Glob Environ Chang 25:121–132

Küchenmeister K, Küchenmeister F, Kayser M, Wrage-Mönnig N, Isselstein J (2013) Influence of drought stress on nutritive value of perennial forage legumes. Int J Plant Prod 7:693–710

Lazri M, Ameur S, Brucker JM, Lahdir M, Sehad M (2015) Analysis of drought areas in northern Algeria using Markov chains. J Earth Syst Sci 124(1):61–70

Lei TJ, Wu JJ, Li XH et al (2015) A new framework for evaluating the impacts of drought on net primary productivity of grassland. Sci Total Environ 536:161–172

Li B, Su H, Chen F, Li H, Zhang R, Tian J, Chen S, Yang Y, Rong Y (2014) Separation of the impact of climate change and human activity on streamflow in the upper and middle reaches of the Taoer River, northeastern China. Theor Appl Climatol 118:271–283

Li XZ, Han GD, Guo CY (2013) Impacts of climate change on dominant pasture growing season in Central Inner Mongolia. Acta Ecol Sin 33(13):4146–4155

Liu ZL, Wang W, Hao DY, Liang CZ (2002) Probes on the degeneration and recovery succession mechanisms of Inner Mongolia steppe. J Arid Land Resour Environ 26:84–91

Lohani VK, Loganathan GV (1997) An early warning system for drought management using the palmer drought index. J Am Water Resources Assoc 33:1375–1386

Mann HB (1945) Non-parametric test against trend. Econometrica 13: 245–259

Marofi S, Soleymani S, Salarijazi M, Marofi H (2012) Watershed-wide trend analysis of temperature characteristics in Karun-Dez watershed, southwestern Iran. Theor Appl Climatol 110(1–2):311–320

Martinez CJ, Maleski JJ, Miller MF (2012) Trends in precipitation and temperature in Florida, USA. J Hydrol 452-453:259–281

McKee TB, Doesken NJ, Kleist J (1993) The relationship of drought frequency and duration to time scales. Paper presented at the applied climatology, Anaheim, CA

Meehl GA, Karl T, Easterling DR et al (2000) An introduction to trends in extreme weather and climate events: observations, socioeconomic impacts, terrestrial ecological impacts, and model projections. Bull Am Meteorol Soc 81:413–416

Michaelides SC, Tymvios FS, Michaelidou T (2009) Spatial and temporal characteristics of the annual rainfall frequency distribution in Cyprus. Atmos Res 94(4):606–615

Mishra AK, Singh VP (2010) A review of drought concepts. J Hydrol 391(1–2):202–216

Naderpour M, Lu J, Zhang G (2014) An intelligent situation awareness support system for safety-critical environments. Decis Ecis Support Syst 59:325–340

Naderpour M, Lu J, Zhang G (2015) An abnormal situation modeling method to assist operators in safety-critical systems. Reliab Eng Syst Safe 133:33–47

Ochola WO, Kerkides P (2003) A Markov chain simulation model for predicting critical wet and dry spells in Kenya: analysing rainfall events in the Kano plains. Irrig Drain 52:327–342

Paulo AA, Ferreira E, Coelho C, Pereira LS (2005) Drought class transition analysis through Markov and Loglinear models, an approach to early warning. Agr Water Manage 77(1–3):59–81

Paulo AA, Pereira LS (2007) Prediction of SPI drought class transitions using Markov chains. Water Resour Manag 21(10):1813–1827

Paulo AA, Pereira LS (2008) Stochastic prediction of drought class transitions. Water Resour Manag 22(9):1277–1296

Peng SZ, Wei Z, Dou CY, Xu JZ (2009) Model for evaluating the regional drought index with the weighted Markov chain and its application. Syst Eng Theory Pract 29:173–178

Purba JH, Lu J, Zhang G, Pedrycz W (2014) A fuzzy reliability assessment of basic events of fault trees through qualitative data processing. Fuzzy Sets Syst 243:50–69

Qi JG, Chen JQ, Wan SQ, Ai LK (2012) Understanding the coupled natural and human systems in dryland East Asia. Environ Res Lett 7:015202

Sheffield J, Wood EF (2012) Drought: past problems and future scenarios. Routledge, Abingdon

Smith LT, Aragão LEOC, Sabel CE, Nakaya T (2014) Drought impacts on children's respiratory health in the Brazilian Amazon. Sci Rep-UK 4

Sneyers R (1990) On the statistical analysis of series of observations. Secretariat of the World Meteorological Organization, Geneva, p 192

Steinemann AC (2006) Using climate forecasts for drought management. J Appl Meteorol Climatol 45:1353–1361

Sun CZ, Zhang Y, Lin XY (2003) Model of Markov chain with weights and its application in predicting the precipitation state. Syst Eng Theory Pract 4(4):100–105

Sun ZY, Zhang JQ, Yan DH, Wu L, Guo EL (2015) The impact of irrigation water supply rate on agricultural drought disaster risk: a case about maize based on EPIC in Baicheng City, China. Nat Hazards 78(1):23–40

Sung JH, Chung E, Kim Y, Lee B (2015) Meteorological hazard assessment based on trends and abrupt changes in rainfall characteristics on the Korean peninsula. Theor Appl Climatol. doi:10.1007/s00704-015-1581-0

Tall A, Patt A G, Fritz S (2013) Reducing vulnerability to hydro-meteorological extremes in Africa. A qualitative assessment of national climate disaster management policies: Accounting for heterogeneity. Weather and Climate Extremes. 1:4–16

Viola F, Liuzzo L, Noto LV, Lo Conti F, La Loggia G (2014) Spatial distribution of temperature trends in Sicily. Int J Climatol 34(1):1–17

Wang HJ, Chen YN, Pan YP, Li WH (2015a) Spatial and temporal variability of drought in the arid region of China and its relationships to teleconnection indices. J Hydrol 523:283–296

Wang W, Zhu Y, Xu RG, Liu JT (2015b) Drought severity change in China during 1961–2012 indicated by SPI and SPEI. Nat Hazards 75(3):2437–2451

Wilhite DA, Glantz MH (1987) Understanding the drought phenomenon: the role of definitions. Vestview Press, Boulder

Wu JD, Li N, Yang HJ, Li CH (2008) Risk evaluation of heavy snow disasters using BP artificial neural network: the case of Xilingol in Inner Mongolia. Stoch Env Res Risk A 22(6):719–725

Xia JZ, Liu SG, Liang SL et al (2014) Spatio-temporal patterns and climate variables controlling of biomass carbon stock of global grassland ecosystems from 1982 to 2006. Remote Sens-Basel 6(3):1783–1802

Yeh C, Wang J, Yeh H, Lee C (2015) SDI and Markov chains for regional drought characteristics. Sustainability-Basel 7(8):10789–10808

Zhang G, Ma J, Lu J (2009) Emergency management evaluation by a fuzzy multi-criteria group decision support system. Stoch Env Res Risk A 23:517–527

Zhang T, Zhang G, Lu J et al (2012) A new index and classification approach for load pattern analysis of large electricity customers. IEEE T Power Syst 27(1):153–160

Zhao F, Xu Z, Huang J (2007) Long-term trend and abrupt change for major climate variables in the upper yellow river basin. Acta Meteorol Sin 21:204–214